Application of interval field method to the stability analysis of slopes in presence of uncertainties

Chengxin Feng[1], Matthias Faes[2], Matteo Broggi[1], and Michael Beer[1,3,4]

[1]Institute for Risk and Reliability, Leibniz University Hannover, Callinstr. 34, 30167 Hannover, Germany email. Email: feng.chengxin@irz.uni-hannover.de
[2]TU Dortmund University, Chair for Reliability Engineering, Leonhard-Euler-Strasse 5, 44227 Dortmund
[3]Institute for Risk and Uncertainty and School of Engineering, University of Liverpool, Liverpool L69 7ZF, UK
[4]International Joint Research Center for Resilient Infrastructure & International Joint Research Center for Engineering Reliability and Stochastic Mechanics, Tongji University, Shanghai 200092, PR China

ABSTRACT

Spatial uncertainty of soil parameters has a significant impact on the analysis of slope stability. Interval field analysis is emerging as a complementary tool of the conventional random field method that can take spatial uncertainty into account, which, however, has not been investigated in slope stability analysis. The present paper proposes a new method, named the interval field limit equilibrium method (IFLEM), for assessing the stability of slope in the presence of the interval field. In this method, the modified exponential function is introduced to characterize the spatial uncertainty of the interval field and the Karhunen-Loève-like decomposition is employed to generate the interval field. Then, in a single calculation, the deterministic slope stability analyzed by the Morgenstern-Price approach is implemented in order to estimate the safety factor. Subsequently, the upper and lower bounds of the interval of safety factor are efficiently evaluated by a kind of surrogate-assisted global optimization algorithms, such as Bayesian global optimization used in this study. Finally, the effectiveness of the proposed method is verified by the numerical example. The results indicate that the proposed method can provide reasonable accuracy and efficiency, which is potentially applicable to a number of geotechnical systems.

INTRODUCTION

Slope failure is a major threat to people's lives and property in mountainous areas. Due to the complex material composition and various deposition conditions, there is considerable spatial uncertainty in the properties of geotechnical materials (Phoon and Kulhawy 1999). Previous studies have indicated that the spatial uncertainty usually has a great impact on the design and analysis of geotechnical structures, hence it should be properly taken into account. The random field theory as one of the feasible techniques to characterize the spatial uncertainty (Griffiths and Fenton 2004). A series of progresses have been emerged in recent decades, particularly a comprehensive overview is given (Jiang et al. 2022). Although the random field theory can address the spatial uncertainties, it requires a large number of samples to obtain statistical characteristics, such as mean value, coefficient of variation, and correlation function. However, it is difficult to estimate these parameters in the presence of sparse measurement data, particularly the correlation length and correlation function (Cami et al. 2020). To address the challenges connected to the statistical inference of the properties of autocorrelation functions, (Wang et al. 2019) proposed a bootstrap method for statistically inferring the autocorrelation coefficients as well other parameters of a random field. However, for sparsely sampled random fields, extra statistical uncertainties are introduced when estimating the sampling distribution of the random field parameters (Montoya-Noguera et al. 2019).

Alternatively to random fields, the interval field method proposed by (Moens et al. 2011) only requires the upper and lower bounds of material parameters, as well as a description of the spatial dependence for modelling the spatial information. As a possibilistic method, the interval field method has rapidly developed in recent years, and a large number of studies have been conducted to compare it with probabilistic random fields. For instance, (Chen et al. 2020) made an objective comparison between the interval and random field methods for the modelling of spatial uncertainty in the case of sparse data. The researchers have shown that the interval field method and the random field method are not competing but complementary. This complementarity was earlier illustrated by (Elishakoff et al. 1994), who compared structural models with initial imperfections via stochastic and nonstochastic models and concluded that if probabilistic information is available, one has to use a probabilistic approach and if the probabilistic information is unavailable, one should use nonstochastic approach for uncertainty quantification. From the preceeding discussion, it can be seen that the interval field method is receiving growing attention, but its application in geotechnical engineering is rarely reported. Therefore, the present study expands its scope on characterizing the spatial uncertainty in geotechnical engineering.

In practical terms, an interval field can be regarded as a family of dependent interval variables indexed by location. When considering this interpretation, the methods developed for propagating interval variables could also be applicable to the propagation of interval fields. Over the past several decades, a plethora of methods have been developed for interval uncertainty propagation, such as the interval arithmetic (Moens and Hanss 2011), the interval perturbation methods (Wang et al. 2014) and the global optimization approach (Deng et al. 2017), etc. It is recommended to refer to (Faes and Moens 2020) for a comprehensive review on the related computational methods. Among these algorithms, global optimization approaches are the standard technique for solving interval problems. In this direction, a Bayesian global optimization is also presented to obtain the lower and upper response bounds of a computationally expansive model subject to multiple interval variables (Dang et al. 2022).

In this paper, the stability analysis of slopes is analyzed when the spatial uncertainty affecting the slopes is modeled by interval fields. The main contributions of this work are summarized as follows: first, the interval field is introduced to characterize the spatial uncertainty of slopes. This is a modelling strategy complementary to the conventionally used random fields, and it is, to the authors' best knowledge, applied to slope stability for the first time. In this representation, an expansion over an orthogonal basis, similar to the Karhunen-Loève-like decomposition in random field analysis, is used to represent the interval field by employing multiple interval variables. Second, a general methodology, called the interval field limit equilibrium method (IFLEM), is proposed to propagate interval fields in slopes. This approach estimates the resulting lower and upper bounds of the safety factor of the slope stability. Additionally, the Bayesian global optimization algorithm is applied to find the lower and upper bounds of the safety factor of a slope characterized by multiple interval variables, where the Morgenstern-Price method is employed for deterministic analysis.

INTERVAL FIELD THEORY

The interval field model solves the problems of changing mechanical parameters with spatial location from a non-probabilistic perspective by measuring the spatial uncertainty of the parameters in the form of upper and lower bounds (Sofi et al. 2019). In this paper, the K-L like expansion is used to represent the interval field $\psi^I(\mathbf{x}) : \Omega \times \mathbb{IR} \mapsto \mathbb{IR}$, with $\mathbb{IR}$ the space of interval valued real numbers. The expansion of an interval field is written as:

$$\psi^I(\mathbf{x}) = \psi_o^I(1 + \psi_n^I(\mathbf{x})), \tag{1}$$

$$\psi_n^I(\mathbf{x}) = \sum_{j=1}^{\infty} \sqrt{\lambda_j} f_j(\mathbf{x}) \zeta_j, \tag{2}$$

where ψ_o^I is the center value of the interval field, $\psi_n^I(\mathbf{x})$ is a dimensionless interval field with unit range, $\lambda_m \in [\,0, \infty)$ is the m-th eigenvalue of the spatial dependency function, $f_m : \Omega \mapsto \mathbb{R}$ is the m-th eigenfunction of the spatial dependency function, and $\zeta_j \in \mathbb{IR}$ is the j-th extra unitary interval (Sofi 2015).

The extra unitary interval is quite different from the classical unitary interval. It relies on the rules of the classical interval analysis. The specific details about the classical interval analysis can be found in (Sofi 2015). The extra unitary interval is given by

$$\zeta_j \in [-1, 1], \; j = 1, 2, \cdots, l. \tag{3}$$

Besides, the uncertain flexibility of the spatial dependency condition is described by a single interval variable constant over the whole range. For that, the following equality holds

$$\zeta_j \times \zeta_j = [0, 1]. \tag{4}$$

For numerical implementation, the interval field is represented by l-term expansions. To be specific, the l-term expansions of the interval field reads

$$\psi^I(\mathbf{x}) = \psi_o^I(1 + \sum_{j=1}^{l} \sqrt{\lambda_j} f_j(\mathbf{x})\zeta_j). \tag{5}$$

For details of the method, the reader is referred to the work of (Sofi et al. 2019). In this process, the error of the l-term expansions of the interval field can be represented as:

$$\varepsilon_{\mathrm{t}}(\psi^I(\mathbf{x})) = 1 - \frac{\sum_{j=1}^{l} \lambda_j}{\sum_{j=1}^{\infty} \lambda_j}, \tag{6}$$

where $\varepsilon_{\mathrm{t}} \in [\,0, \infty)$ is the error of the l-term expansions of the interval field, λ_j is j-th eigenvalue.

In this paper, the $\gamma(\mu, \upsilon)$ is used to characterize spatial uncertainty and has a number of formulations, such as the single exponential model, squared exponential model, etc (Cami et al. 2020). Among them, the modified exponential model is differentiable at the origin, such that the K-L expansion itself exhibits higher computational efficiency (Spanos et al. 2007; Faes et al. 2022). Thus, in this paper, we assumed that the spatial dependency function, $\gamma(\mu, \mu', \upsilon, \upsilon')$, has the following modified exponential form:

$$\gamma(\mu, \mu', \upsilon, \upsilon') = \exp\left(-\frac{|\mu - \mu'|}{l_{\mathrm{h}}} - \frac{|\upsilon - \upsilon'|}{l_{\mathrm{v}}}\right)(1 + \frac{|\mu - \mu'|}{l_{\mathrm{h}}})(1 + \frac{|\upsilon - \upsilon'|}{l_{\mathrm{v}}}), \tag{7}$$

where $\gamma(\mu, \mu', \upsilon, \upsilon')$ is the spatial dependency function, (μ, υ) and (μ', υ') denote two points in a 2-D space, $\exp(\cdot)$ is the exponential function, l_{h} is the horizontal spatial dependency length which is similar to the horizontal correlation distance, l_{v} is the vertical spatial dependency length which is similar to the vertical correlation distance, $|\mu - \mu'|$ and $|\upsilon - \upsilon'|$ respectively denote the horizontal and vertical distances between the two points.

In this paper, an assumed spatial dependency function, the modified exponential function is used for illustrative purpose. After the spatial dependency function $\gamma(\mu, \mu', \upsilon, \upsilon') : \Omega \times \Omega \mapsto \mathbb{R}$ is determined, the spatial uncertainty can then be characterized (Faes et al. 2022). Specifically, the Fredholm integral equation of the second kind is solved to obtain the eigenvalues and eigenfunctions of the $\gamma(\mu, \mu', \upsilon, \upsilon')$ (Atkinson and Han 2009). The Fredholm integral equation of the second kind takes the form:

$$\int_{\Omega} \gamma(\mu, \mu', \upsilon, \upsilon') f_j(\mu', \upsilon') \mathrm{d}\mu' \mathrm{d}\upsilon' = \lambda_j f_j(\mu, \upsilon), \tag{8}$$

where λ_j is the j-th eigenvalue of the spatial dependency function, and $f_j(\cdot)$ is the j-th eigenfunction of the spatial dependency function. In order to numerically solve the Fredholm integral equation of the second kind, the interval field is first discretized into a series of points, and the integral Eq. (8) is solved by determining the eigenvalues and eigenvectors of the covariance matrix.

INTERVAL FIELD LIMIT EQUILIBRIUM METHOD

Limit equilibrium method and its extension to interval field

The limit equilibrium method (LEM) used in this paper is the Morgenstern-Price method. The Morgenstern-Price method is similar to the Spencer method, but it allows for various user-specified interslice force functions (Morgenstern and Price 1965). In the Morgenstern-Price method, it is assumed that

$$\chi_1/e_1 = \tan\beta = \lambda f(u), \tag{9}$$

where χ_1 is inter-slice vertical force, e_1 is inter-slice horizontal force, λ is a constant, and f is an inter-slice function. In particular, the inter-slice functions in the present implementation is half-sine function.

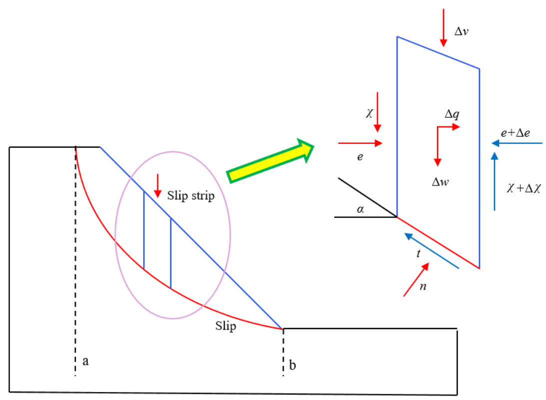

Fig. 1. Schematic diagram of limit equilibrium method

According to Fig. 1, the equilibrium equations of the forces in the horizontal and vertical directions are derived respectively. In the process, cohesion and internal friction angle are expressed in the form of interval fields. The obtained equations are shown as follows:

$$t\sin\alpha + n\cos\alpha = \Delta w + \Delta v - \Delta\chi, \tag{10}$$

$$t\cos\alpha - n\sin\alpha = \Delta q - \Delta e, \tag{11}$$

$$t\cos\alpha = \psi_c^I \Delta p \sec\alpha + n\tan\psi_\varphi^I, \tag{12}$$

where t is tangential force at the bottom of the soil strip, n is the normal force at the bottom of the soil strip, α is the angle between the tangent line at the bottom of the soil strip and the horizontal direction, Δw is the gravity of the soil strip, Δv is the external force on the soil strip in the vertical direction, $\Delta\chi$ is the difference in vertical force between strips on both sides of the soil strip, Δq is the horizontal component of the soil strip, Δe is the difference in horizontal force between strips on both sides of the soil strip, ψ_c^I is the interval field of c, and ψ_φ^I is the interval field of φ.

In addition, the equilibrium equation of the moment is derived as follows

$$(\chi + \Delta\chi)\frac{\Delta p}{2} + \chi\frac{\Delta p}{2} + (e + \Delta e)\Delta q - e\Delta r - \Delta q\Delta s = 0, \tag{13}$$

where Δp is the width of the soil strip, e is the lower soil strip is subjected to the horizontal force between the strips of the upper soil strip, Δr is the distance between the position of the force of the upper soil strip on the lower soil strip and the center point of the bottom of the strip, and Δs is the distance between the position of the horizontal component of the soil strip and the center of the bottom of the strip. The f_s of the slope can be calculated from Eqs. (14) and (15) by combining Eqs. (10)-(13) according to the equilibrium condition of force and moment, that is,

$$-\frac{\mathrm{d}e}{\mathrm{d}p}(1+\tan\psi_\varphi^I\tan\alpha)+\frac{\mathrm{d}\chi}{\mathrm{d}p}(\tan\psi_\varphi^I-\tan\alpha)=\psi_c^I\sec^2\alpha+(\frac{\mathrm{d}w}{\mathrm{d}p}+\frac{\mathrm{d}v}{\mathrm{d}p})$$
$$(\tan\psi_\varphi^I-\tan\alpha)-\frac{\mathrm{d}q}{\mathrm{d}p}(1+\tan\psi_\varphi^I\tan\alpha), \tag{14}$$

$$\int_a^b[\lambda f(p)e-e\tan\alpha]\,\mathrm{d}p=\int_a^b\frac{\mathrm{d}q}{\mathrm{d}p}\Delta s\,\mathrm{d}p. \tag{15}$$

Estimate the safety factor bounds by Bayesian global optimization

In this paper, we use an improved Bayesian global method to determine the upper and lower bounds of the interval, i.e., the maximum and minimum values (Dang et al. 2022). In this problem, the optimization problem, including the maximum and minimum values, can be formulated as

$$\begin{cases} \max\ f_s(\boldsymbol{\zeta}) \\ \min\ f_s(\boldsymbol{\zeta}) \\ \text{s.t. } \zeta_j\times\zeta_j=[0,1], \end{cases} \tag{16}$$

where $\boldsymbol{\zeta}=(\zeta_1,\zeta_2,\cdots,\zeta_l)^{\mathsf{T}}$ is the l-dimensional vector of interval variables, $f_s(\boldsymbol{\zeta}):\mathbb{IR}^l\mapsto\mathbb{IR}$ is the objective function, and $\zeta_j\times\zeta_j=[0,1]$ is the constraint conditions.

For the minimization problem, the objective function improvement $\theta(\boldsymbol{\zeta})$ is defined as

$$\theta(\boldsymbol{\zeta})=\max\{\gamma_{\min}-\hat{\gamma}(\boldsymbol{\zeta}),0\}, \tag{17}$$

where $\gamma_{\min}$ is the current optimal objective function value, and $\hat{\gamma}(\boldsymbol{\zeta})$ is the set of parameters that obey normal distribution.

The expectation value of $\theta(\boldsymbol{\zeta})$ is given by (Jones et al. 1998)

$$\mathbb{E}[\theta(\boldsymbol{\zeta})]=\begin{cases}(\gamma_{\min}-\hat{\gamma}(\boldsymbol{\zeta}))\Phi(\frac{\gamma_{\min}-\hat{\gamma}(\boldsymbol{\zeta})}{s(\boldsymbol{\zeta})})+s(\boldsymbol{\zeta})\phi(\frac{\gamma_{\min}-\hat{\gamma}(\boldsymbol{\zeta})}{s(\boldsymbol{\zeta})}),\ s>0\\ 0,\ s=0,\end{cases} \tag{18}$$

where $\mathbb{E}[\cdot]$ is the expectation operator, Φ is the standard normal cumulative distribution function, ϕ is the standard normal distribution probability density function, $\hat{\gamma}(\boldsymbol{\zeta})$ and $s(\boldsymbol{\zeta})$ are the mean and standard deviation of the normal distribution of the Kriging model predictions, respectively.

The new sample points are found by solving the following suboptimization problem which maximize the value of $\mathbb{E}[\theta(\boldsymbol{\zeta})]$:

$$\begin{cases}\max\limits_{\boldsymbol{\zeta}}\ \mathbb{E}[\theta(\boldsymbol{\zeta})]\\ \text{s.t. } \zeta_j\times\zeta_j=[0,1].\end{cases} \tag{19}$$

Convergence criterion for Bayesian global optimization

The convergence criterion is an essential element for the optimization algorithm. It is determined by controlling the ratio of the maximum expected value of $\theta(\zeta)$ to the current optimal objective function value. The convergence criterion of the present paper is defined as

$$\frac{|\max\,\mathbb{E}[\theta(\zeta)]|}{|\gamma_{\min}|+\delta} \leq \epsilon, \tag{20}$$

where $\max\,\mathbb{E}[\theta(\zeta)]$ represents the maximum value of $\mathbb{E}[\theta(\zeta)]$, $\gamma_{\min}$ represents the minimum value of γ observed so far, δ is an infinitesimal value, ϵ is the threshold value. In this case, δ is 1e-6 and ϵ is 0.001. The optimization process is terminated when the ratio of the maximum expected value of $\theta(\zeta)$ to the current optimal objective function value is less than ϵ for three successive iterations.

ILLUSTRATIVE EXAMPLES

Description of the problem

To illustrate, a single-stage slope is used to demonstrate the generation of the interval field, and then the interval of the f_s is calculated according to the proposed method. This slope has a height of 28 m and an angle of 36.9°, in which the height of the lower floor is 4 m and the height of the upper floor is 24 m, as shown in Fig. 2. In order to generate interval fields for the slope, 489 elements are discrete in the slope. In the process, the c and φ are spatially variable described by the interval fields which are generated by the method mentioned in Section 2. And we use the parameter of midpoint of the element on behalf of the whole element.

It is crucial to determine the upper and lower boundaries of the interval field and the parameters of the spatial dependence function when establishing the interval field. This is because interval estimation captures the uncertainty of the parameters through an upper bound with a lower bound. The initial estimation of interval boundaries can be based on the analyst's expertise and experimental data. However, the expert knowledge that is available in most practical engineering design cases is sparse, ambiguous, or subjective. In such cases, it is wise to collect more data to refine the interval. A Bayesian inference scheme can in this context be used to determine interval bounds on small data sets. It is based on considering a complete set of parameterized probability density functions to determine the likelihood function, which can then be used in a Bayesian framework to assess the extreme value distributions on the bounds of the interval, given the available data. The parameters of the interval field of the slope are shown in Table 1. The minimum value of c is 15 kPa and the maximum value is 21 kPa, and the minimum value of φ is 16° and the maximum value is 24°. The horizontal spatial dependency length l_h is set to 30 m, and the vertical spatial dependency length l_v is 4 m.

Interval field analysis results and discussion

First, the interval field of the single-stage slope is generated and the error of the K-L like expansion level is analyzed. In this example, the error of the K-L like expansion is controlled within 5% and the K-L like expansion term is six (Huang et al. 2001). Then,

Table 1
Material parameters of the single-stage slope in Example 1

Parameters	Maximum value	Minimum value	l_h	l_v
c(kPa)	21	15	30	4
φ(°)	24	16	30	4

the eigenfunctions and eigenvalues are solved according to the spatial dependency function.

The single-stage slope with interval field is calculated and its sliding surfaces (SS) are obtained as shown in Fig. 2. To calculate the f_s, the sliding surfaces should be selected first. For illustration purposes, three typical sliding surfaces are considered. In this figure, three special sliding surfaces are marked according to the range of the f_s. The red sliding surface in the diagram represents the most dangerous sliding surface, while the green sliding surface represents the safest sliding surface. Each sliding surface was analyzed respectively. The safety factor bounds of the upper and lower of the single-stage slope with interval field are calculated by the Bayesian global optimization method. The interval of f_s was obtained as [0.83, 0.994] for the sliding surfaces 1, [0.946, 1.132] for the sliding surfaces 2, and [1.107, 1.415] for the sliding surfaces 3. The calculated interval of f_s is represented in Fig. 3. The optimization of the sliding surface 1 to obtain the interval of f_s required 19 deterministic analyses, the sliding surface 2 required 20 times, and the sliding surface 3 required 21 times. In Table 2, the results of the Bayesian global optimization are compared with the surrogate optimization method. It can be found that Bayesian global optimization shows great advantages in terms of both computational accuracy and efficiency. For the sliding surface 2 of interval field analysis, the interval of f_s is [0.946, 1.132]. Since $f_s = 1$ is included in the interval of the f_s, the stability of the slope in this state is unsure, and essentially no fixed statement can be made. This is because there is no information available on the probability distribution of the c and φ within the bounds of the interval. In the analysis by the interval method, only the information of the upper and lower boundaries of c and φ are predicted.

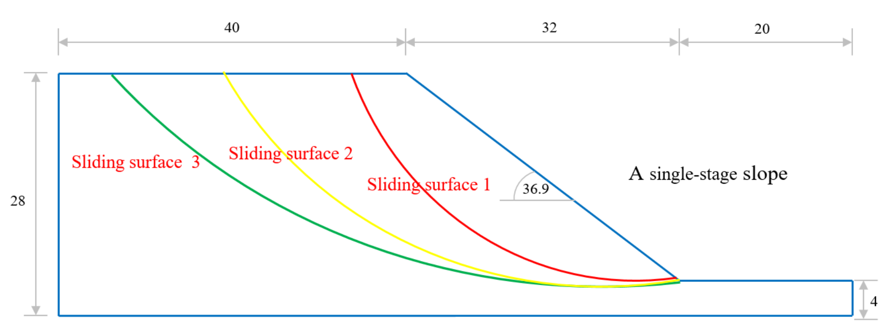

Fig. 2. Three typical sliding surfaces for the single-stage slope failure

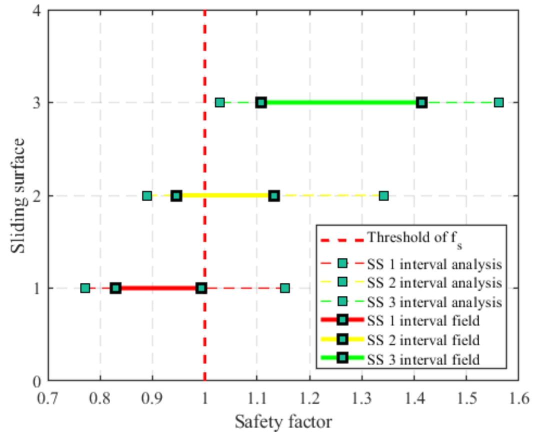

Fig. 3. Results of interval field and interval analysis in the single stage slope analysis

Table 2
Results of the efficiency comparison

Method	Result	*N*
Bayesian optimization	[1.107, 1.415]	21
Surrogate optimization	[1.011, 1.412]	505 + 368

For the same c and φ intervals, the interval field with consideration of spatial uncertainty is compared with the interval analysis method for homogeneous materials. The intervals of f_s were calculated for the interval field and interval analysis, respectively. It can be found in Fig. 3. It can be noticed that the interval field method can reduce the interval of f_s in comparison with the interval analysis method. Moreover, it is more consistent with the real situation after considering the spatial uncertainty.

In order to study the influence of interval field parameters on the calculation results, the influence of spatial dependency length on the calculation results of the interval field is analyzed. It's shown in Figs. 4 and 5. The interval fields were calculated for the horizontal spatial dependency lengths of 5 m, 10 m, 15 , 20 m, 25 m, and 30 m, respectively. The interval fields were calculated for the vertical spatial dependency lengths of 2 m, 4 m, 6 , 8 m, and 10 m, respectively. When the horizontal spatial dependency length is 5 m, the interval of the calculated results is [1.198, 1.341]. And the interval of the calculated results is [1.107, 1.415] when the horizontal spatial dependency length is 30 m. With the expansion of the input parameter interval, the interval of the calculated f_s increases rapidly. When the spatial dependency length is greater than 25m, the percentage of the interval increase of the f_s becomes larger. Therefore, more attention should be paid to the selection of the spatial dependency length.

CONCLUDING REMARKS

The main contribution of this work is the proposal of a new interval field limit equilibrium method, IFLEM, for efficiently estimating the interval of the f_s of a slope

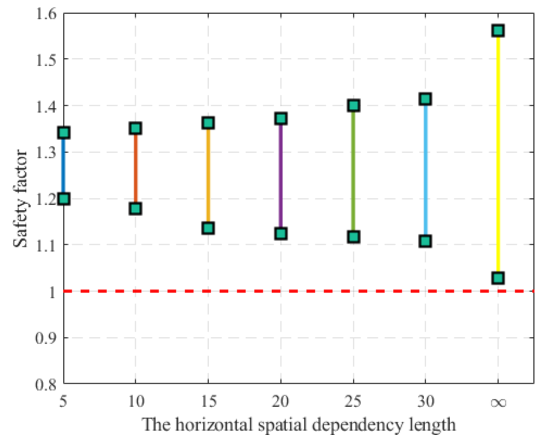

Fig. 4. Influence of the horizontal spatial dependency length on interval field results

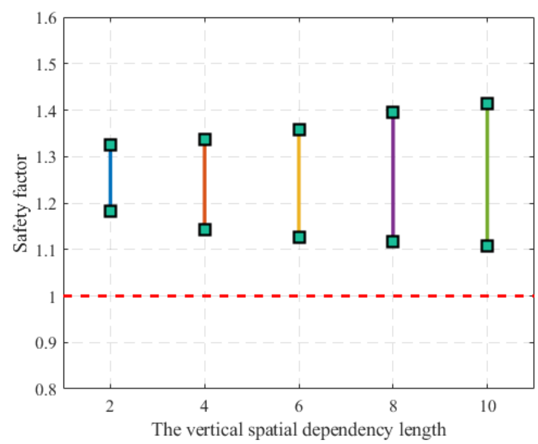

Fig. 5. Influence of the vertical spatial dependency length on interval field results

in the presence of spatial uncertainty. For our purpose, the IFLEM method first characterizes the interval field by using the Karhunen-Loève like expansion. Further, based on the Morgenstern-Price method and the generated interval field (IF), a computational method for calculating the f_s of slopes is proposed. Then, to efficiently and accurately solve the optimization problem for the upper and lower bounds of the f_s, a dedicated iterative algorithm is developed based on Bayesian global optimization (BGO). Finally, the IFLEM is formed by an elegant combination of IF and LEM. The main feature of IFLEM is the ability to obtain the interval of the f_s, resulting from uncertainties in model parameters and their spatial uncertainty. The numerical example is presented to illustrate the availability and effectiveness of the proposed approach.

The numerical results indicate that the proposed method allows to perform the uncertainty analysis of slopes in the presence of sparse data. Noting that the upper and lower bounds of the f_s are obtained with a small number of deterministic analyses, the proposed method seems to be effective and efficient for quantitative analysis of slopes with scarce data. The influences of the spatial dependency length and the interval radius are investigated. The results shows that different values of spatial dependency length can result in a large variation of the interval of f_s. Besides, compared to the interval radius of c, the interval of f_s is more sensitive to the interval radius of φ. Hence, it is of great significance to reasonably determine the spatial dependency length and the interval radius of φ in the interval field analysis of slopes.

REFERENCES

Atkinson, K. and Han, W. (2009). "Numerical solution of fredholm integral equations of the second kind." *Theoretical Numerical Analysis*, Springer, 473–549.

Cami, B., Javankhoshdel, S., Phoon, K.-K., and Ching, J. (2020). "Scale of Fluctuation for Spatially Varying Soils: Estimation Methods and Values." *ASCE-ASME Journal of Risk and Uncertainty in Engineering Systems, Part A: Civil Engineering*, 6(4), 03120002.

Chen, Z.-Y., Imholz, M., Li, L., Faes, M., and Moens, D. (2020). "Transient landing dynamics analysis for a lunar lander with random and interval fields." *Applied Mathematical Modelling*, 88, 827–851.

Dang, C., Wei, P., Faes, M. G., Valdebenito, M. A., and Beer, M. (2022). "Interval uncertainty propagation by a parallel Bayesian global optimization method." *Applied Mathematical Modelling*, 108, 220–235.

Deng, Z., Guo, Z., and Zhang, X. (2017). "Interval model updating using perturbation method and radial basis function neural networks." *Mechanical Systems and Signal Processing*, 84, 699–716.

Elishakoff, I., Cai, G., and Starnes Jr, J. (1994). "Non-linear buckling of a column with initial imperfection via stochastic and non-stochastic convex models." *International Journal of Non-Linear Mechanics*, 29(1), 71–82.

Faes, M. and Moens, D. (2020). "Recent trends in the modeling and quantification of non-probabilistic uncertainty." *Archives of Computational Methods in Engineering*, 27(3), 633–671.

Faes, M. G., Broggi, M., Spanos, P. D., and Beer, M. (2022). "Elucidating appealing features of differentiable auto-correlation functions: A study on the modified exponential kernel." *Probabilistic Engineering Mechanics*, 103269.

Griffiths, D. V. and Fenton, G. A. (2004). "Probabilistic Slope Stability Analysis by Finite Elements." *Journal of Geotechnical and Geoenvironmental Engineering*, 130(5), 507–518.

Huang, S., Quek, S., and Phoon, K. (2001). "Convergence study of the truncated Karhunen-Loève expansion for simulation of stochastic processes." *International Journal for Numerical Methods in Engineering*, 52(9), 1029–1043.

Jiang, S.-H., Huang, J., Griffiths, D., and Deng, Z.-P. (2022). "Advances in reliability and risk analyses of slopes in spatially variable soils: A state-of-the-art review." *Computers and Geotechnics*, 141, 104498.

Jones, D. R., Schonlau, M., and Welch, W. J. (1998). "Efficient Global Optimization of Expensive Black-Box Functions." *Journal of Global Optimization*, 13(4), 455–492.

Moens, D., De Munck, M., Desmet, W., and Vandepitte, D. (2011). "Numerical dynamic analysis of uncertain mechanical structures based on interval fields." *IUTAM symposium on the vibration analysis of structures with uncertainties*, Springer, 71–83.

Moens, D. and Hanss, M. (2011). "Non-probabilistic finite element analysis for parametric uncertainty treatment in applied mechanics: Recent advances." *Finite Elements in Analysis and Design*, 47(1), 4–16.

Montoya-Noguera, S., Zhao, T., Hu, Y., Wang, Y., and Phoon, K.-K. (2019). "Simulation of non-stationary non-Gaussian random fields from sparse measurements using Bayesian compressive sampling and Karhunen-Loève expansion." *Structural Safety*, 79, 66–79.

Morgenstern, N. u. and Price, V. E. (1965). "The analysis of the stability of general slip surfaces." *Geotechnique*, 15(1), 79–93.

Phoon, K.-K. and Kulhawy, F. H. (1999). "Characterization of geotechnical variability." *Canadian Geotechnical Journal*, 36(4), 612–624 Publisher: NRC Research Press.

Sofi, A. (2015). "Structural response variability under spatially dependent uncertainty: stochastic versus interval model." *Probabilistic Engineering Mechanics*, 42, 78–86.

Sofi, A., Romeo, E., Barrera, O., and Cocks, A. (2019). "An interval finite element method for the analysis of structures with spatially varying uncertainties." *Advances in Engineering Software*, 128, 1–19.

Spanos, P. D., Beer, M., and Red-Horse, J. (2007). "Karhunen-Loève expansion of stochastic processes with a modified exponential covariance kernel." *Journal of Engineering Mechanics*, 133(7), 773–779.

Wang, C., Qiu, Z., Wang, X., and Wu, D. (2014). "Interval finite element analysis and reliability-based optimization of coupled structural-acoustic system with uncertain parameters." *Finite Elements in Analysis and Design*, 91, 108–114.

Wang, Y., Zhao, T., and Phoon, K.-K. (2019). "Statistical inference of random field auto-correlation structure from multiple sets of incomplete and sparse measurements using Bayesian compressive sampling-based bootstrapping." *Mechanical Systems and Signal Processing*, 124, 217–236.